

CYCLIC PLASTIC BEHAVIOR AND FATIGUE LIFE OF AZ91 ALLOY IN AS-CAST AND ULTRAFINE-GRAINED STATE

Stanislava Fintová^{1, 2, 3,*}, Ludvík Kunz²

¹ CEITEC – Central European Institute of Technology, Brno University of Technology, Technická 3058/10, 61600 Brno, Czech Republic

² Institute of Physics of Materials Academy of Sciences of the Czech Republic, v. v. i., Žitkova 22, 616 62 Brno, Czech Republic

³ University of Žilina, Faculty of Mechanical Engineering, Univerzitná 1, 010 26 Žilina, Slovak Republic

*corresponding author: tel: +420 541 212 301, e-mail: fintova@ipm.cz.

Resume

Fatigue properties of magnesium alloy AZ91 in as-cast and in ultrafine-grained state prepared by equal channel angular pressing were investigated. The fatigue strength in the low-cycle fatigue region was found to be substantially improved by the severe plastic deformation, whereas the improvement in the high-cycle fatigue region is negligible. The cyclic plastic response in both states is qualitatively similar; short initial softening is followed by a long cyclic hardening. The observed fatigue behavior was discussed in terms of specific microstructural features of both states and on the basis of cyclic slip localization and fatigue crack initiation.

Article info

Article history:

Received 22 December 2013

Accepted 23 February 2014

Online 15 September 2014

Keywords:

AZ91;

ECAP;

Bimodal structure;

Fatigue;

Plastic deformation;

Crack initiation.

Available online: <http://fstroj.uniza.sk/journal-mi/PDF/2014/16-2014.pdf>

ISSN 1335-0803 (print version)

ISSN 1338-6174 (online version)

1. Introduction

AZ91 magnesium alloy, the most popular magnesium alloy from AZ group, exhibits perfect castability and good mechanical properties combined with good corrosion resistance (for high purity version of the alloy) and low production costs. Because this alloy has been used in industry since more than eighty years [1] its mechanical and corrosion behaviour has been thoroughly investigated in the past and the results can be found in plenty of papers, e.g. [2 - 6] Beyond the favourable properties the alloy has also some disadvantages consisting mainly in its poor formability and limited ductility at room temperature. This is a natural consequence of its hexagonal close packed (hcp) structure with restricted number of available slip systems and presence of an intermetallic phase $Mg_{17}Al_{12}$ [2 - 4, 7 - 10].

Within the last some years the alloy, primarily intended for castings, has been investigated with the aim to answer the question if severe plastic deformation (SPD) can influence its tensile strength, σ_{UTS} , yield stress, σ_y , and, particularly, improve the ductility due to the grain refinement. One of the most popular SPD techniques is equal channel angular pressing (ECAP). In the case of magnesium alloys the ECAP treatment has to be done at elevated temperatures by reason of activation of more slip systems in the hcp structure. Otherwise undesirable cracks appear in the processed material. It has been shown that the ultimate strength and ductility of AZ91 alloy can be significantly improved by ECAP treatment. The improvement of σ_{UTS} , σ_y and ductility of AZ91 is more significant when compared to the other AZ magnesium alloys.

This is a consequence of high amount of small $Mg_{17}Al_{12}$ particles after ECAP [7, 11]. Besides the mechanical properties also corrosion resistance of magnesium alloys can be improved by ECAP treatment [3, 8].

The fatigue life of the cast AZ91 alloy expressed in terms of S-N curve can be found in literature, e.g. [4, 12] and the same holds for its cyclic stress-strain behaviour expressed in terms of cyclic softening/hardening curves. The S-N curve exhibits a sharp knee. The slope of the S-N curve in the region of high number of cycles to failure is extremely low and the fatigue limit is in the range from 60 to 85 MPa, according to the details of chemical composition and casting process. The cyclic stress-strain behaviour of the cast material [12] exhibits at the beginning a weak cyclic softening (for some tens to hundreds of loading cycles), which is followed by cyclic hardening. In the case of higher applied stress amplitudes the maximum on the cyclic softening/hardening curves is missing and the cyclic hardening is characteristic response for the whole fatigue life.

As far as to the authors' knowledge no experimental data on the fatigue strength and the stress-strain response of the AZ91 after ECAP are available. The main aim of this study was to experimentally determine the S-N curve and the cyclic stress-strain response and to compare them with the behaviour of as-cast alloy. Simultaneously the influence of ECAP treatment on the microstructure was examined. The manifestation of localization of cyclic plasticity and formation of early fatigue cracks on the surface was examined by scanning electron microscopy (SEM).

2. Material and experiments

Fatigue behavior and the response of the material to the cyclic deformation were investigated on AZ91 alloy in as-cast and in ultrafine-grained (UFG) state, which was prepared by severe plastic deformation by ECAP. The severe plastic deformation was

conducted at temperature 573 K. The intersecting angle of the die channels was 120°. The processing route was Bc. The billets were manufactured by 6 passes. Final semi-products for machining of specimens for fatigue tests were cylindrical rods of 80 mm length and 15 mm in diameter. ECAP treatment was applied directly to the material in as-cast state.

The basic mechanical properties of the cast and UFG material are the following: $\sigma_{UTS} = 167 \pm 8$ MPa, the yield stress $\sigma_{0.2} = 87 \pm 8$ MPa and ductility 3.1 ± 0.4 % for material in as-cast state and $\sigma_{UTS} = 321 \pm 21$ MPa, $\sigma_{0.2} = 160 \pm 4$ MPa and the ductility 5.4 ± 4.7 % for the material after several plastic deformation by ECAP. Chemical composition of the AZ91 magnesium alloy is shown in Table 1.

Cylindrical specimens, Fig. 1, with the gauge length 15 mm and the gauge length diameter 4 mm were used for fatigue tests. The specimen gauge length was carefully ground and subsequently polished to get smooth surface for the observation by SEM with the aim to reveal the development of slip bands and cracks.

Fatigue testing was performed under controlled load in symmetrical tension-compression (load ratio $R = -1$). The direction of the loading of UFG material coincided with the extrusion direction. For the fatigue tests servohydraulic testing system Shimadzu EHF-F1 was used. During the first 50 cycles the test frequency was 0.1 Hz. Then it was increased to 1 Hz until 100 cycles were reached. After 500 cycles the test frequency was increased to 5 Hz. After elapsed 3000 cycles the frequency was increased to 10 Hz. At the pre-defined number of cycles the hysteresis loops were recorded; for this purpose during the recording procedure the loading frequency was reduced to 0.1 Hz. When the specimen lifetime exceeded 1×10^6 cycles, the specimen was moved to a resonant fatigue machine Amsler HFP 5100 and the loading was continued with a frequency of about 60 Hz. Tests were conducted at room temperature in laboratory air.

Table 1

Chemical composition of AZ91 magnesium alloy (in wt. %).									
elements	Al	Zn	Mn	Si	Fe	Be	Ni	Cu	Mg
wt. %	8.7	0.65	0.25	0.006	0.003	0.0008	0.0006	0.0005	Rest

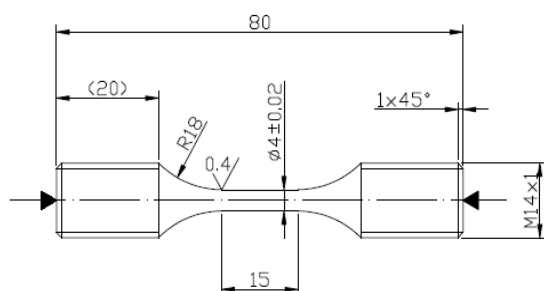


Fig. 1. Geometry of specimen for the fatigue tests.

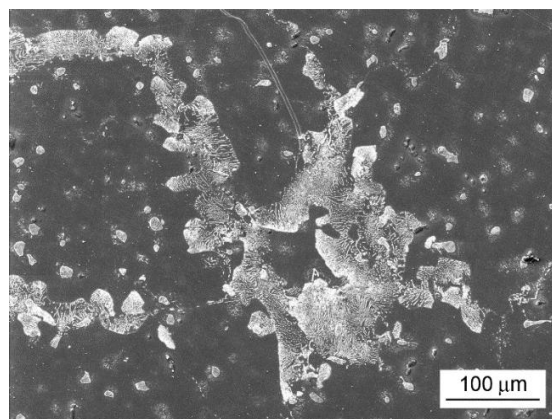
Microstructure and the specimen surface were examined by SEM Tescan LYRA 3 XMU FEG/SEM x FIB.

3. Results

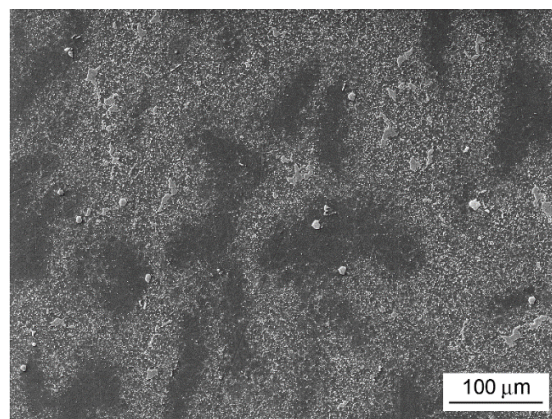
The microstructure of AZ91 magnesium alloy in as-cast state consists of a solid solution of alloying elements in magnesium and eutectic. Eutectic consists of the solid solution and particles of intermetallic phase $Mg_{17}Al_{12}$ in a plate like shape. Furthermore, large primary $Mg_{17}Al_{12}$ and AlMn based particles are present in the structure, Fig. 2a.

The structure after ECAP processing by 6 passes by the route Bc is not fully homogenous from the macroscopic point of view. It can be characterized as bimodal. There are areas with small grains with the average grain size of $3.3 \pm 0.5 \mu m$ with large amount of small $Mg_{17}Al_{12}$ particles, and areas with larger grains, with the average grain size of $9.9 \pm 4.5 \mu m$ where the density of small $Mg_{17}Al_{12}$ particles is low. Some large primary $Mg_{17}Al_{12}$ particles and AlMn based particles remained in the heavily deformed structure, Fig. 2b. The grain size deviates from the convention that as UFG materials are considered those ones having the grain size in the range from 1000 to 100 nm. On the other

hand, materials prepared by ECAP are generally denoted as UFG. In the case of Mg alloys ECAP produces substantially smaller grain size as can be reached by conventional deformation techniques like rolling etc. That is why in this work the authors stick on the description of the microstructure as UFG.



a) Microstructure of cast AZ91 alloy



b) Microstructure of AZ91 after ECAP

Fig. 2. Microstructure of cast AZ91 alloy and after ECAP. SEM, etched by 2% Nital.

Results of the experimental determination of the fatigue life of AZ91 in the as-cast state and after ECAP are shown in Fig. 3. Obviously, there is a strong influence of ECAP procedure on the S-N curves. Cast AZ91 magnesium alloy exhibits typical knee in the S-N curve. Stress amplitude 80 MPa can be considered to be the

endurance limit (based on 10^7 cycles) for the cast alloy. Below this stress amplitude the fatigue life of all specimens tested exceeded 10^7 cycles. All the specimens loaded at higher stress amplitudes than 80 MPa failed before they reached 10^5 cycles. The decreasing part of the S-N curve can be well fitted by the power law dependence

$$\sigma_a = 282 N_f^{-0.11} \quad (1)$$

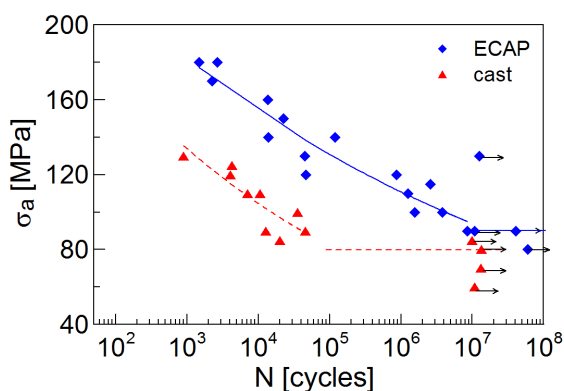


Fig. 3. S-N curves of cast AZ91 alloy and after ECAP.
(full colour version available online)

The S-N curve of the UFG alloy is shifted to the higher lifetimes at the same stress amplitudes when compared to the cast alloy. It decreases linearly with the increasing number of cycles in the log-log plot and can be well approximated by the following equation

$$\sigma_a = 300 N_f^{-0.07} \quad (2)$$

There is no knee on the S-N curve of the UFG material. From the comparison of both curves it is obvious that the improvement of the fatigue properties by ECAP is substantial only in the low-cycle fatigue region. The endurance limit based on 10^7 cycles for the alloy processed by ECAP is 90 MPa, which is very close to the endurance limit of the cast alloy.

The cyclic deformation curves determined under load control are shown in Fig. 4. At the beginning of cycling the AZ91 in the as-cast

state exhibits a short stage of the cyclic softening during a few of cycles. The softening is followed by a pronounced cyclic hardening, which is characteristic for the decisive part of the fatigue life. The effect of initial cyclic softening is more apparent at low stress amplitudes. With increasing stress amplitudes the maximum on the softening/hardening curves is shifted towards lower number of cycles and became less expressive.

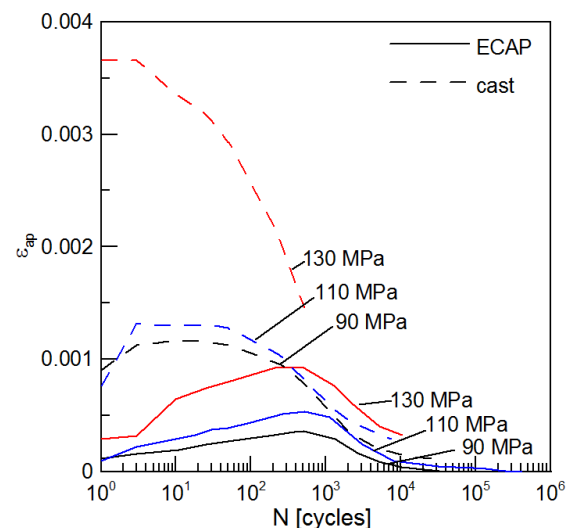


Fig. 4. Cyclic deformation curves of cast AZ91 alloy and after ECAP.
(full colour version available online)

The cyclic deformation curves of UFG material are qualitatively similar to those of the cast alloy. The length of the initial cyclic softening stage of UFG structure is somewhat longer than that of the cast alloy and makes typically some hundreds of cycles. After the maximum is reached, a long stage of the cyclic hardening represents the characteristic stress-strain response. In the case of material treated by ECAP cyclic softening was typical for the beginning period up to approximately 10^3 cycles. This period was followed by cyclic hardening, which was not as strong as in the case of the cast material. The effect of cyclic softening was largest for the specimen tested at 130 MPa. Also in this case the cyclic hardening represents the largest part of the ECAPed material fatigue life.

4. Discussion

The structure of AZ91 alloy processed by ECAP was found to be bimodal even after 6 passes of ECAP. The bimodality could be caused by missing pretreatment of the alloy before severe plastic deformation. A heat treatment is usually applied before the ECAP process. It makes the structure homogeneous and the following ECAP processing then refines the structure. Chen et al. [11] found that the heat treatment and subsequent ECAP resulted in creation of well-developed UFG structure after 2 ECAP passes. The following passes caused than only homogenization of the UFG structure. In the case when the pretreatment is missing the structure obtained by six ECAP passes by the route Bc can remain heterogeneous as observed in this study.

The effect of ECAP on the improvement of tensile properties and ductility of AZ91 was found to be more expressive than in the case of other AZ magnesium alloys [3, 7, 8, 11]. The explanation is sought in dominantly larger amount of small $\text{Mg}_{17}\text{Al}_{12}$ particles and also in the strengthening role of the fine grain structure [5]. Gubicza et al. [13], observed significant improvement of strength and ductility of AZ91 alloy after only 2 ECAP passes at 543 K despite of not homogeneous final microstructure. The explanation is based on the evolution of precipitates during ECAP. Following ECAP passes led to little or no additional improvement of material strength. The results of this work and published data indicate that also the bimodal structure results in serious improvement of tensile properties, which is comparable with the fully homogenous UFG microstructure. The improvement of ultimate stress σ_{UTS} observed in this study for the bimodal structure of AZ91 alloy obtained by ECAP, was 100% when compared to the as-cast state. Chung et al. [5, 7] observed 100% improvement of tensile strength of AZ 91 processed by ECAP. In their case the obtained microstructure after 6 passes through the die at

593 K [7] and 573 K [5] was homogenous with $8\text{ }\mu\text{m}$ [7] and $6\text{ }\mu\text{m}$ [5] the average grain size.

Fatigue strength of AZ91 was substantially improved by ECAP in the low-cycle fatigue region, Fig. 3. This is obviously related to the high σ_{UTS} and σ_y of the bimodal structure. Contrary to the low-cycle fatigue region the fatigue strength improvement in the high-cycle fatigue region is negligible. There is no significant difference in the endurance limit of the cast alloy and the alloy after ECAP. The S-N curve of the cast alloy has the typical knee at 10^5 cycles. Observation of surface relief development during cycling implies the following explanation. The cracks initiate mainly on slip bands created due to the cyclic plastic deformation in softer solid solution areas. Fatigue cracks which were found in eutectics apparently grew into these regions from the solid solution. Sometimes broken intermetallic $\text{Mg}_{17}\text{Al}_{12}$ particles were observed, however the cracks did not propagate further into their surroundings. With decreasing stress amplitude the percent occurrence of created slip bands rapidly decreases. At the stress amplitude of about 85 MPa the slip band formation in softer solid solution areas ceases entirely and the lifetime exceeds 10^7 cycles. On run-out specimens no slip bands were observed. The stress amplitude of 85 MPa can be considered as threshold amplitude for slip band formation. This conclusion was supported by SEM observation of specimens gauge length prepared by polishing and etching.

In the case of ECAPed alloy two mechanisms of fatigue crack initiation were observed. Slip bands in large grains of the bimodal structure were preferable places for crack initiation. The process has the same features as in the cast material; only the scale is smaller. Besides this mechanism crack initiation at grains boundaries in small grained areas was observed, particularly at lower stress amplitudes. However, the decisive majority of the investigated fracture surfaces bear witness

for initiation of fatal fatigue cracks in large grains of the bimodal structure. Nevertheless, it can be expected, that with decreasing stress amplitude the transition from initiation at slip bands to initiation on grain boundaries and on cracked large precipitates can take place. The confirmation of this idea needs further experimental evidence.

The experimentally determined response of the cast AZ91 alloy on the cyclic deformation, Fig. 4, consists in a short initial softening followed by continuous cyclic hardening. This is in full agreement with the results published by Wolf et al. [12], who observed cyclic softening for 10^2 cycles and following cyclic hardening which was typical for the largest part of the fatigue life. When the experiments are performed under total strain control [6], the cyclic hardening follows the preliminary softening which lasts typically $1 - 2 \times 10^3$ cycles. Plastic deformation of cast material occurs mainly in softer solid solution dendrites where slip bands were observed. The length of the observed slip bands is limited only by areas of solid solution. The cracks initiated in slip bands later grow perpendicularly to the loading direction. Slip bands were not observed in the eutectic hardened by the intermetallic phase $Mg_{17}Al_{12}$ in a plate like shape. In the eutectic areas only cracked intermetallic $Mg_{17}Al_{12}$ particles were observed, however, these cracks did not grow further into the dendrite areas. This observation is in agreement with Wolf et al. [12] who observed the crack initiation on slip bands formed in the solid solution areas and on structural defects which were present in the structure. In the alloy studied in this work no structural defects were observed.

The short initial softening of AZ91 after ECAP can be attributed to a relaxation of stresses in the heavily deformed structure. The following cyclic hardening, Fig 4, is related mainly with the cyclic slip activity within the large grained areas of the bimodal structure with the average grain size of $9.9 \pm 4.5 \mu m$ where the

density of small $Mg_{17}Al_{12}$ particles is low. These areas exhibit similar behavior as the solid solution areas in cast material; only their dimension is substantially smaller. SEM observation reveals development of slip bands during cycling, inherently at higher stress amplitudes. Similar behavior was mentioned by Chung et al. [5] for unidirectional loading of bimodal structure of AZ91 alloy. They observed formation of slip bands at the beginning of loading in large favorably oriented grains and later on onset of plastic deformation of grains in small grained areas. Cyclic plastic deformation of large grains was proved in the present study by development of slip bands on which cracks were initiated, Fig. 5b. With decreasing stress amplitude the number of slip bands decreases. Below 120 MPa no slip band formation was observed on specimen gauge length. Simultaneously, the plastic strain amplitude in high-cycle region had become non-measurable (below 10^{-6}).

The slip activity in the small grained areas manifests itself by formation of slip bands very sporadically. This indicates that the contribution of small grained areas to the plastic strain amplitude and its changes during cycling seems to be very low.

5. Conclusions

ECAP treatment of cast AZ91 improves its mechanical properties and fatigue strength in low-cycle fatigue region. The improvement in high-cycle fatigue region is negligible and the fatigue strength is similar to that of the cast material. Cyclic stress-strain response of ECAPed alloy is qualitatively the same as the response of cast alloy, namely short initial cyclic softening followed by long cyclic hardening.

The microstructure of AZ91 alloy processed by ECAP by 6 Bc passes is bimodal. The cyclic slip activity manifests itself mainly in the coarse grained areas of the structure, where long slip bands and later fatigue cracks form. The role and contribution of coarse grained areas to the

fatigue damage is decisive in the low-cycle region. Its cyclic plasticity resembles that of as cast material. With increasing number of cycles and exhausting of cyclic hardening in coarse grained regions the cyclic deformation in fine grained areas becomes important.

They are later on sites of initiation of fatigue cracks. With decreasing stress amplitude the slip activity in grain boundary crack initiation mechanism starts to play the dominant role.

Acknowledgment

The Czech Science Foundation under the contract 108/10/2001 and Ministry of Education of the Czech Republic under the projects CZ.1.07/2.3.00/30.0039 and 7AMB14SK064 supported this work. The research is supported by European regional development fund and Slovak state budget by the project ITMS 26220220121 (50%).

References

- [1] H. Altwicker et al.: Magnesium und seine Legierungen, J. Springer Verlag, Berlin, 1939.
- [2] A. Němcová, J. Zapletal, M. Juliš, T. Podrábský: Mat. Eng. Vol. 16 (4) (2009) 5-10.
- [3] L. Bukovinová, B. Hadzima: Corr. Eng. Sci. Technol. 47(5) (2012) 352-357
- [4] G. Eisenmeier, B. Holzwarth, H.W. Höppel, H. Mughrabi: Mat. Sci. Eng. A319-321 (2001) 578-582.
- [5] C.W. Chung, R.G. Ding, Y.L. Chiu, W. Gao: J. Phys.: Conf. Ser. 241 (2010) 012101.
- [6] B. Ebel-Wolf, F. Walther, D. Eifler: Mat. Sci. and Eng. A 486 (2008) 634-640.
- [7] C.W. Chung, R.G. Ding, Y.L. Chiu, M.A. Hodgson, W. Gao: IOP Conf. Series: Mat. Sci. and Eng. 4 (2009) doi:10.1088/1757-899X/4/1/012012.
- [8] B. Hadzima, M. Janeček, P. Suchý, J. Müller, L. Wagner: Mat. Sci. Forum 584-586 (2008) 994-999.
- [9] B. L. Mordike, T. Ebert: Mat. Sci. Eng. A302 (2001) 37-45.
- [10] K.N. Braszczynska-Malik, Precipitates of γ -Mg17Al12 Phase in AZ91 Alloy, In: http://cdn.intechopen.com/pdfs/12741/InTech-Precipitates_of_gamma_mg17al12_phase_in_mg_al_alloys.pdf
- [11] B. Chen, D.L. Lin, L. Jin, X.Q. Zeng, Ch. Lu: Mat. Sci. Eng. A483-484 (2008) 113-116.
- [12] B. Wolf, C. Fleck, D. Eifler.: Int. J. Fat 26 (2007) 1357-1363.
- [13] J. Gubicza, K. Máthis, Z. Hege: J. of Alloys and Compounds 492 (2010) 166-172.